

SCALE-DEPENDENT ANALYSIS OF IONOSPHERE FLUCTUATIONS

Stéphane G. Roux, Patrice Abry

Physics Dept., ENS Lyon
CNRS, UMR5672, France
firstname.lastname@ens-lyon.fr

Petra Koucká Knížová, Zbyšek Mošna

Institute of Atmospheric Physics,
ASCR, Czech Republic,
pkn@ufa.cas.cz

ABSTRACT

Ionosphere consists of a large complex systems whose analysis is of major importance, e.g., for climatology or radio-communications. Therefore, studying its variations, usually analyzed in terms of long-term trends versus short-term fluctuations, as well as the mechanisms driving them is of importance. This contribution hence performs a scale-dependent cross-analysis of the F2-region critical frequency data, locally measured at 11 mid-latitude European stations, and 5 global solar and geomagnetic indices. It shows that such Ionospheric variations are well described by the superimposition of well-defined long-term cycles with highly correlated fractional Gaussian noise fluctuations. Also, it is shown that mid-latitude European stations display highly correlated variations even for short-term fluctuations and that, while the solar activity mostly drives long-term cycles, short-term fluctuations are essentially controlled by the geomagnetic activity.

Index Terms— Ionosphere Fluctuations, Multiresolution Analysis, Wavelet Coherence, Scale Invariance.

1. INTRODUCTION

Ionosphere. Ionosphere denotes the ionized upper part of the atmosphere, where free electrons exist at high enough density to have a significant influence on the propagation of radio frequency electromagnetic waves. Ionosphere consists of a large natural system showing a high variability over a broad range of scales, from minutes (with, for instance, Traveling Ionospheric Disturbances) to years (reflecting, for instance, solar cycle activities). It is characterized in terms of electron densities, which usually leads to the distinction of three regions (D, E, and F), defined by inflection points in electron density profiles, yielding distinct signatures in the radio wave spectrum, reflected by the Ionosphere [1].

Ionospheric Fluctuations. There has been continuous and on-going interests and efforts to analyze Ionospheric fluctuations and it is nowadays widely accepted that the solar and geomagnetic activities constitute the main drivers for the ionospheric variability, although meteorological causes may also contribute [2]. It is, for instance, well-known that ionospheric disturbances and storms follow geomagnetic disturbances. Also, the analysis of the long-term variations is considered more and more important as they are suspected to potentially contribute to global climatological changes.

Along another line, Ionospheric short-term fluctuations also play an important control on electromagnetic wave propagation and hence influence significantly navigation and telecommunication systems. Many attempts were hence performed to measure correlations between geomagnetic or solar indices and ionospheric variability (cf. e.g., [3], and reference therein) and to derive models for ionospheric fluctuation predictions (cf. [4] for a review of such models and limitations). However, the understanding of the causes for Ionospheric fluctuations remains unsatisfactory and further characterizations of Ionospheric fluctuations are largely needed.

Long-term versus short-term. Implicitly, the description of Ionospheric fluctuations above assumes natural the classical split of the analysis of variability into *long-term* versus *short-term* variations, as sketched in Fig. 1 (a). *Long-term* usually refers to time scales larger than the year, often well defined by characteristic strong periodicities such as the 11-year solar cycle, the 1-year Earth cycle, etc. *Short-term* in turn, is implicitly understood as the range of scales finer than the long-term ones, and is hence far less grounded on well-recognized obvious periodicities. A number of works were dedicated to the *detection* of *physically relevant structures* with short-term characteristic scales, hence permitting to associate the *short-term* fluctuations to founding physical mechanisms. This is notably the case in [5] (and references therein), where it is concluded that structures corresponding to all *short-term* scales can actually be identified in foF2 measurements. This observation constitutes the founding motivation for undertaking the scale dependent analysis proposed here.

Goals, contributions and outline. While each Ionospheric regions shows its own variability, the interest for the analysis of the F2-Region has recently been growing (cf. e.g., [6]), because of its role in Earth environment and space weather. Also, the F2-region remains present both over daytime and night-time, a fact of major practical interest for radio-communications and navigation. In this context, the present work aims at contributing to the statistical characterization of F2-Region electron concentration variabilities, proposing to replace the classical long term versus short term separation by a scale dependent cross-analysis. The large ionosphere and global indices data sets analyzed here are described in Section 2. Ionospheric fluctuations are first studied based on the usual long term versus short term separation by means of classical spectrum estimation and cross-covariance (cf. Section 3). This motivates the need of a scale dependent (or multiresolution) description of the Ionospheric fluctuations, based on wavelet spectra and wavelet coher-

Work supported by the joint Grant from French CNRS and Czech ASCR Grant # 18098. P. Koucká Knížová is grateful to L'Oreal for the Women in Science Award.

ence functions. This is depicted in Section 4, together with the benefits of scale dependent cross analysis for Ionosphere analysis.

2. DATA SETS

Volume and chronology. The data sets analyzed consists of 5 global solar and geomagnetic indices as well as 11 local measurements, collected daily, from 1971 until 1998. The typical sample size is hence roughly $\simeq (5 + 11) \times 10000$.

foF2 measurements. Ionospheric sounding refers to a technology that enables physicists to obtain vertical profile of plasma frequency. The maxima on the profile are called critical frequencies and the fluctuations of the critical foF2 frequency accounts for the electron concentration fluctuations. For this study, daily (taken as a median around noon) measurements of the F2-region critical frequency, foF2, are collected over 11 mid-latitude (ranging from 45° to 65°) European stations. This hence enables to examine latitude dependences in analysis, an important issue as Ionosphere fluctuations are expected to vary greatly with geographical locations (polar, auroral, mid-latitudes, and equatorial zones). A representative example is illustrated in Fig. 1 (a).

Global geomagnetic and solar indices. The global Earth geomagnetic activity is usually quantified via several indices, amongst which the physicists involved in the present study selected Kp, Dst and AE, because they can account for geomagnetic changes equally under quiet or strongly disturbed circumstances. While the former belongs to the general K-family, the two latter indices are designed to target specific and different parts or characteristics of the Earth magnetic field behavior. The solar activity is measured by the counts of the number of active spots at the Sun surface (SSN) as well as the solar radio flux per unit frequency at a wavelength of 10.7 cm, near the peak of the observed solar radio emission, referred to as the F10.7 parameter. These two indices constitute the longest available direct record of solar activity. For further details on the definitions or measurements of these indices, the reader is referred to e.g., [2].

3. TRENDS VERSUS FLUCTUATIONS

Classical spectrum estimation is first applied to all time series independently using the standard Welch Periodogram estimation procedures (with a blackmann window of size 3 years and a 50% overlap).

Long-term cycles. The estimated Power Spectral Density (PSD) is displayed in Fig. 1 (b), for a representative station, in Fig. 1 (a). It clearly shows the one-year period, together with two other periodicities close to 180 and 120 days, understood by physicists, as higher order harmonics of the fundamental one-year period, induced by the numerous non linear mechanisms entering the equations governing Ionospheric plasma variabilities. Interestingly, a characteristic cycle with period close to 28 days is also visible, which is related to the Sun rotation.

Short-term scale invariance. The key interesting finding here being that beyond this 28-day period, i.e. at finer scales or shorter-term, no specific scale can be singled out or considered as characteristics. This therefore lead to propose that fine scale fluctuations are not driven by physical

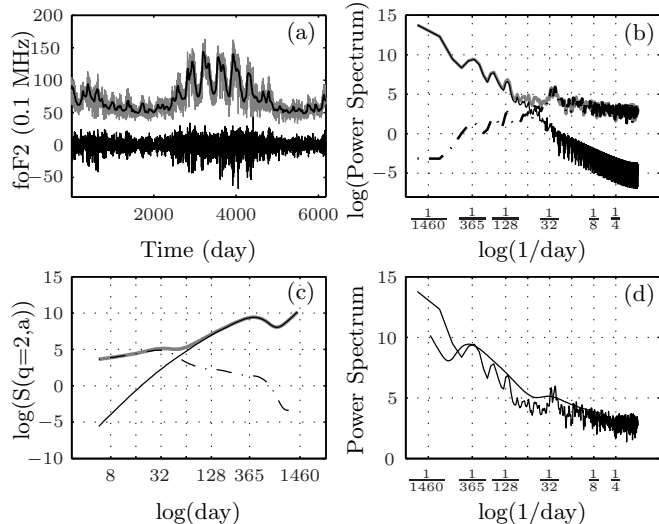


Fig. 1. Trends and fluctuations. Moscow: (a) raw data (gray), trend (solid) and fluctuations (dashed), (b) corresponding power spectra; (c) Wavelet Spectra; (d) Classical and wavelet Spectra superimposed.

mechanisms with specific time scales but instead account for the superimposition of a collection of mechanisms occurring randomly at all scales ranging from the day (current lower data resolution) to the month. One can suspect that this mechanism holds for coarse scales up to 120 days, though here masked by the superimposition of the 28-day period. This analysis suggests that the fine scales (equivalently the high frequencies) of the data can be modeled by a second-order stationary $1/f$ -process: $\Gamma_X(\nu) \sim C|\nu|^{-\gamma}$, $|\nu| \rightarrow +\infty$. This situation is referred to as *scale invariance*, or *scaling*, and implies that, instead of focusing on specific cycles, one should determine mechanisms that relate scales together ; this further motivates the use of a scale dependent (or multiresolution) analysis, based on wavelet decomposition.

Trends versus fluctuations. From a practical perspective, splitting *long-term* from *short-term* fluctuations amounts to decomposing the time series X to analyze into trend X_a and details X_d : $X(t) = X_a(t) + X_d(t)$. X_a is obtained by low-pass filtering X with a Blackmann window, while X_d is obtained by difference. The common usage in the discipline together with the spectral analysis described above and the heuristic considerations reported in Section 1, led us to choose a size of 64 days for the Blackmann window, this arbitrariness being further discussed below. The corresponding signals X_a and X_d and their PSD are superimposed in Fig. 1. It shows, unsurprisingly, that the trend X_a captures the well-established coarse scales periodicities, while the details X_d essentially describes the scale invariance regime. Yet, it illustrates unambiguously that scale invariance is not caused by non-stationarities or trends in data, that mimic a scaling properties, as commonly but erroneously written in the literature: Instead, trends and scaling exist independently in two different ranges of scales and are superimposed.

Cross-correlation. The correlation coefficient, $\rho = \frac{(X - \bar{X})(Y - \bar{Y})}{\sqrt{(X - \bar{X})^2} \sqrt{(Y - \bar{Y})^2}}$, is used to assess cross-correlation between two stationary signals X and Y ,

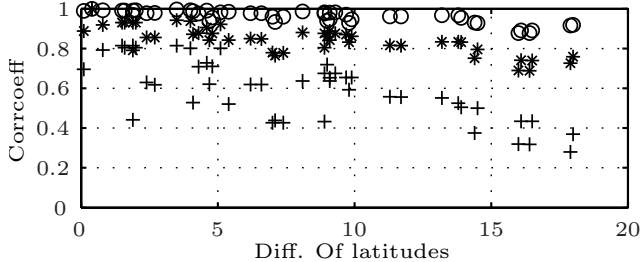


Fig. 2. Correlation versus latitude difference. for raw data (*), trend (o) and fluctuations around the trend (+).

where $\bar{X} = \frac{1}{N} \sum_{i=1}^N X_i$ denotes the sample mean estimate, while $(X - \bar{X})^2$ is the standard sample variance estimate. Practically, the estimate $\hat{\rho}$ of ρ is obtained by averaging estimates obtained from 50% overlapping sliding windows, each window being roughly 3-years long.

foF2 measurements. Correlation coefficients estimated from all pairs of foF2 measurements are shown in Fig. 2 (*), as a function of the difference of latitudes between the station locations. It can be seen that $\hat{\rho}$ remains very high for all pairs, and it can be suspected that this is due to the common trends. Therefore, ρ are also estimated on all pairs of trends and details. As expected, trends are found to be highly correlated (cf. Fig. 2 (o)), indicating a common and single external driving forcing globally these trends. More surprisingly, the details, or short-term fluctuations, are found to remain positively and strongly correlated, even though the correlation coefficients tend to decrease when the difference in latitude increases (cf. Fig. 2 (+)). This indicates that, for these mid-latitudes stations, there are common physical phenomena that drives not only the long-term variations but also the short-term fluctuations.

	SSN	F10.7	Dst	AE	Kp	foF2
SSN		0.84 0.94	-0.08 -0.22	-0.07 -0.45	0.03 0.19	0.43 0.56
F10.7	0.68		-0.14 -0.28	0.03 0.12	0.04 0.11	0.51 0.64
Dst	0.00	-0.05		-0.19 -0.06	-0.66 -0.71	0.06 -0.31
AE	0.05	0.01	-0.22		0.20 0.20	-0.06 -0.16
Kp	0.00	0.00	-0.66	0.19		-0.18 0.03
foF2	0.14	0.19	0.35	0.02	-0.33	

Table 1. Correlation coefficients. Top right triangle: raw data and trends (in bold font); Bottom left: fluctuations. For foF2 data, $\hat{\rho}$ is averaged over the 11 stations.

foF2 measurements vs. global indices. Table 1 reports $\hat{\rho}$ between the indices and the foF2 measurements, for raw data, trends and details. It shows that the two solar indices are highly correlated, in trends and indices, whereas the three geomagnetic indices are weakly cross-correlated, except for Dst and Kp that are found anti-correlated. This is consistent with the observation that a decrease of Dst announce the beginning of the geomagnetic disturbance, and that Kp described the level of disturbance. Solar and geomagnetic in-

indices are found to be uncorrelated. For foF2 measurements, the long-term trends are strongly correlated to the solar indices, while short-term fluctuations are found to be rather correlated to the geomagnetic indices (positively to Dst and negatively to Kp). Interestingly, while Dst appears to be not correlated with foF2, for raw data, it turns out that trends are significantly anti-correlated while short-term fluctuations are equally significantly but positively correlated. This latest example naturally calls into question the arbitrariness of the chosen scale for the separation of short-term fluctuations and long-term variations: How would the results obtained above be changed if the characteristic split scale had been chosen different? This question can be better addressed by defining a scale dependent analysis.

4. SCALE DEPENDENT ANALYSIS

Wavelet transform. Let ψ denote an oscillating, band-pass, pattern well-located jointly in time and frequency, referred to as the mother wavelet. The wavelet coefficients of the signal X are obtained as inner products, $T_X(a, t) = \langle X, \psi_{a,t} \rangle$ between X and dilated and translated templates of $\psi_{a,t}(u) = \psi((u-t)/a)/\sqrt{a}$. The chosen mother wavelet is here a second derivative of a Gaussian function.

Wavelet Spectrum. It has been shown [7] that, when X is a second-order stationary process with spectrum Γ_X , $\mathbb{E}T_X(a, t)^2 = \int \Gamma_X(\nu) a |\tilde{\psi}(a\nu)|^2 d\nu$, where $\tilde{\psi}$ denotes the Fourier transform of ψ . Because $S(a) = \sum_{k=1}^{n_a} T_X(a, k)^2 / n_a$ constitute an estimator for $\mathbb{E}T_X(a, t)^2$, $S(a)$ can be read as a wavelet spectrum: i.e., a measure of the frequency content of X around frequency ν_0/a (where ν_0 is a constant that depends on the choice of ψ). Fig. 1 (c) illustrates this wavelet spectrum and show that it can be superimposed to and compared against to the classical spectrum (d).

Scale invariance. While the wavelet spectrum does not identify well marked periodicities as the Classical spectrum does, it is of particular interest for the analysis of scale invariance. If $\Gamma_X(\nu) \simeq C|\nu|^{-\gamma}$, $|\nu| \rightarrow +\infty$, then $S(a) \simeq |a|^{\gamma+1/2}$, $|a| \rightarrow 0$ [7]. And it has been shown that the estimation of the γ parameters is more accurate when based on the wavelet spectrum than when based on the classical spectrum [7]. The estimated $\gamma = 2H - 1$ are obtained by linear regression in a $\log a$ vs. $\log S(a)$ diagram, performed over scales ranging from 1 to 27 days. For the global indices, the estimated H are reported in Table 2, while for foF2 measurements, it takes the average value of $\hat{H} = 0.94$. Short term fluctuations in Ionosphere can hence be modeled by a highly correlated fractional Gaussian noise, and hence significantly differ from a white noise uncorrelated fluctuation, which likely betrays the existence of a physical mechanisms structuring these fluctuations.

	SSN	F10.7	Dst	AE	Kp	foF2
H	1.58	1.90	1.00	0.88	0.74	0.94

Table 2. Scaling parameters.

Wavelet coherence function. To further analyze scale dependent cross-correlations amongst indices and foF2 measurements, one can defined a wavelet based counterpart of

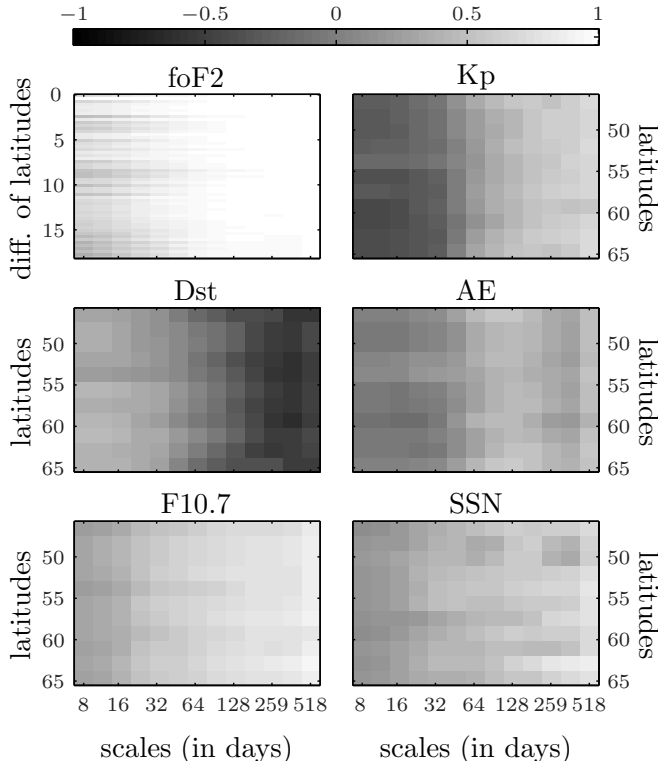


Fig. 3. Wavelet coherence vs. latitudes. x-axis: log of scales (in days), y-axis: latitudes (or difference of latitudes for the top left plot).

the coherence function between X and Y (cf. e.g., [8]):

$$\rho(a) = \frac{\overline{(T_X(a, \cdot) - \overline{T_X(a, \cdot)})(T_Y(a, \cdot) - \overline{T_Y(a, \cdot)})}}{\sqrt{\overline{(T_X(a, \cdot) - \overline{T_X(a, \cdot)})^2}} \sqrt{\overline{(T_Y(a, \cdot) - \overline{T_Y(a, \cdot)})^2}}}, \quad (1)$$

which consists of a correlation coefficients at scale a (equivalently at frequency ν_0/a).

Wavelet coherence estimates are reported in Fig. 3, where the x-axis corresponds to log of the scales ($\log a$) in days, the y-axis to the latitude or the difference in latitude.

It shows that, for foF2 measurements, scales above 64 days are quasi perfectly correlated, indicating that one (or a few) global mechanism drives them all consistently and that scales below 64 days remain strongly correlated ($\rho(a) > 0.5$) whatever the difference in latitudes, which also suggest that short term fluctuations are also driven by a global single mechanism.

The estimated $\rho(a)$ between foF2 measurements and solar indices (cf. Fig. 3 bottom row) appear to increase linearly with $\log a$, roughly from 0.2 at the fine scales to 0.9 at the coarse scales. This confirms that the solar activity is essentially a driver for the long-term fluctuations and that its influence decreases regularly at finer scales.

For the geomagnetic indices, (cf. Fig. 3 middle row and top right), the estimated $\rho(a)$ show clear changes in sign around the 44-day scale. While Kp is negatively correlated below and positively above, this is the converse for Dst. This clearly suggests that Negative ionospheric storms [2] are the most probable scenarios for the Ionospheric response to the

geomagnetic disturbances. Again, these results are found uniformly for all latitudes indicating that short-term fluctuations as much as long-term trends are governed by global mechanisms affecting all mid-latitudes stations consistently.

5. DISCUSSION AND FUTURE WORKS

Combining a large high quality data sets to a multiresolution (scale dependent) cross-correlation analysis enabled to obtain a number of significant conclusions with respect to the analysis of foF2 fluctuations. First, they can be well described by the superimposition of well-defined (solar and earth) cycles with highly correlated fractional Gaussian noise type fluctuations. Second, for the mid-latitudes stations studied here, fluctuations are highly correlated, not only in their long-term trends, as may have been expected, but also for their short-term scale invariant fluctuations, there is hence little benefits in their joint observations. Third, while the scale separating long-term from short-term may seem an arbitrary choice, the use of a wavelet coherence function proposed here, enables to analyze the impact of the solar and geomagnetic activities jointly at all scales. Interestingly, this showed that while the solar activity is mostly controlling long-term trends, it is less and less influent at fine scales. Conversely, the geomagnetic activity influence both short-term fluctuations and long-term trends but in opposite directions. This suggests that the variations of foF2 can be predicted in a scale dependent manner, by the prediction of their wavelet coefficients, for example as: $T_X(a, t) = \sum_i \rho_{X, Y_i}(a) T_{Y_i}(a, t)$, where Y_i would be the F10.7, Kp and Dst indices. This is under current investigations.

6. REFERENCES

- [1] Kenneth Davis, *Ionospheric Radio*, Peter Peregrinus Ltd, London, UK, 1990.
- [2] G. W. Prolss, *Physics of the Earth's space environment: an introduction*, Springer, 2004.
- [3] P. G. Richards, "Seasonal and solar cycle variations of the ionospheric peak electron density: Comparison of measurement and models," *Journal Of Geophysical Research-Space Physics*, vol. 106, no. A7, pp. 12803–12819, 2001.
- [4] A. V. Mikhailov, B. A. de la Morena, G. Miro, and D. Marin, "A method for f(0)f(2) monitoring over spain using the el arenosillo digisonde current observations," *Annali Di Geofisica*, vol. 42, no. 4, pp. 683–689, 1999.
- [5] J. Lastovicka, P. Krizan, P. Sauli, and D. Novotna, "Persistence of the planetary wave type oscillations in fof2 over europe," *Annales Geophysicae*, vol. 21, no. 7, pp. 1543–1552, 2003.
- [6] H. Rishbeth and M. Mendillo, "Patterns of f2-layer variability," *Journal Of Atmospheric And Solar-Terrestrial Physics*, vol. 63, no. 15, pp. 1661–1680, 2001.
- [7] P. Abry, P. Gonçalvès, and P. Flandrin, *Wavelets, spectrum estimation and 1/f processes*, chapter 103, Springer-Verlag, New-York, 1995, *Wavelets and Statistics, Lecture Notes in Statistics*.
- [8] B. Whitcher, P. Guttorp, and D. Percival, "Wavelet analysis of covariance with application to atmospheric time series," *Journal of Geophysical Research - Atmospheres*, 2000.